Oxidation Behaviors of Two Phase NiAl+Ni_3Al Intermetallic Compounds

SangYul Lee, Jung-Suk Lee, JongHoon Lee*, and SangYong Lee**

Department of Materials Engineering, Hankuk Aviation University, KoYang, KyungKi-Do, 412-791, Korea
**High Temperature Materials Group, ** Metal Working & Plasticity Group, Korea Institute of Machinery and Metals Changwon, KyungNam, 641-010*

(Received March 25, 2000; final form May 22, 2000)

ABSTRACT

Improvement of toughness of the brittle intermetallics was reported by controlling the morphologies of the Ni_3Al phase through the solution and aging treatment in two phase NiAl+Ni_3Al alloy. In this work, oxidation behaviors of two phase NiAl+Ni_3Al intermetallic compounds were studied while paying special attention to the early stage oxidation behaviors as well as to the effect of boron addition. Experimental results from oxidation testing at 1100 °C in air flowing at the rate of 70cc/min showed that both types of intermetallic compounds with and without boron addition showed general parabolic oxidation behavior, but addition of boron to the two phase NiAl+Ni_3Al intermetallic compounds deteriorated the oxidation resistance. The differences in the oxidation resistance between the intermetallic compounds with and without boron addition could be attributed to the microstructural difference, in that an accelerated oxidation along the thin layer of Ni_3Al at the grain boundary observed in the Ni-32at.%Al-0.5at.%B intermetallic compound was responsible for the poor oxidation resistance, compared with the Ni-32at.%Al intermetallic compound showing no grain boundary Ni_3Al phase. In the early stage, quite complex oxidation behaviors involving several types of oxide such as NiO, $NiAl_2O_4$, θ-Al_2O_3, α-Al_2O_3 phases were observed, depending upon the location at the grain boundary regions in the Ni-32at.%Al-0.5at.%B intermetallic compound.

INTRODUCTION

Ever since an improvement in the fracture toughness of nickel aluminide through precipitation of rod-like Ni_3Al in an over-saturated NiAl matrix was reported by Russell *et al.* /1/, similar efforts are being made extensively to develop nickel aluminides with good mechanical properties for structural applications /2-7/. Also the addition of a small amount of boron to Ni-32at.%Al two phase NiAl+Ni_3Al alloy was reported to improve extensively both room temperature compressive fracture strength and compressive fracture strain /5/. However much less information is available on the oxidation behaviors of two phase NiAl+Ni_3Al nickel aluminides. In particular the effect of boron addition on the oxidation properties of the two phase NiAl+Ni_3Al intermetallic has yet to be reported, although it is of great interest.

In this study, the isothermal oxidation behaviors of two phase NiAl+Ni_3Al alloy with and without boron addition were defined in terms of microstructure and weight change as a function of oxidation time at 1100°C.

EXPERIMENTAL

Alloys with compositions of Ni-32at.%Al and Ni-32at.%Al-0.5at.%B were produced using a vacuum arc melting furnace and casted into a copper mold. Then alloys were homogenized at 1300°C for 14 hours in an argon atmosphere and were cooled by water quenching. Coupons of 8x6x3 mm were cut and the specimen surface was polished using successively finer SiC papers up to No. 2000 and cleaned ultrasonically in acetone before oxidation.

Isothermal oxidation tests at 1100°C for up to 100 hours were performed under air flowing at a rate of 70 cc per minute. Weight change as well as microstructural examination was carried out using SEM, and EDS analysis was done using Oxford Link ISIS with Li-doped Si window at an accelerating voltage of 20kV. The quantitative analysis was made using ZAF method. A diffractometer using CuKα radiation was used for XRD analysis.

RESULTS AND DISCUSSION

Microstructures of solutionized Ni-32at.%Al alloy consisted of a martensitic β'-NiAl phase as shown in Fig. 1a) and 1b). Addition of 0.5at.%B to Ni-32at.%Al alloy induced a quite drastic microstructural change as shown in Fig. 1c) and 1d). After solutionization followed by water quenching, martensitic NiAl phase formed within the grains while a thick film layer with approximately 20μm in thickness formed at the

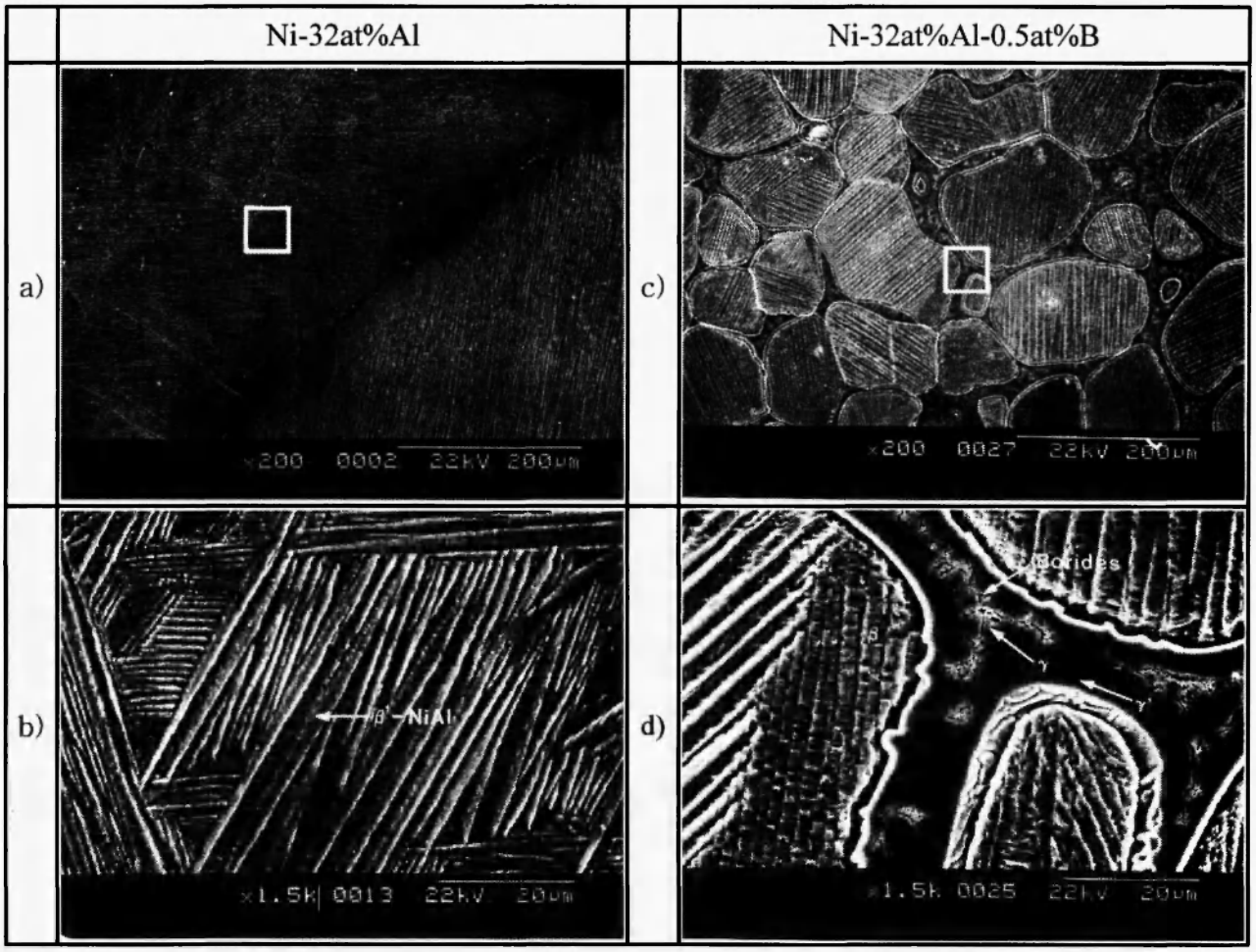

Fig. 1: SEM micrographs of a,b) Ni-32at.%Al and c,d) Ni-32at.%Al-0.5at.%B solutionized at 1300°C for 14hours, b) □ area in a), d) □ area in c)

interface. This film was reported to consist of Ni_3Al phase, Ni solid solution and boride as shown in Fig. 1d) in previous publications /7,8/

Weight change per unit area after isothermal oxidation at 1100°C for up to 100 hours in air flowing at the rate of 70cc/minute is shown in Fig. 2. Both alloys showed a general parabolic oxidation behavior while Ni-32at.%Al alloy showed a much better oxidation resistance than Ni-32at.%Al-0.5at.%B alloy. This could be explained in terms of microstructural difference between two alloys. Excellent oxidation resistance is expected in Ni-32at.%Al alloy as it mainly consisted of NiAl phase, but in Ni-32at.%Al-0.5at.%B alloy thick film of Ni_3Al and other phases formed at the interface and an accelerated oxidation along thick film at the interface as well as depletion of Al at the surface resulted in a reduced oxidation resistance in the Ni-32at.%Al-0.5at.%B alloy. Residual thermal stress as well as microvoids developed between the surface oxides and the matrix induced crack formation at the interface and the surface oxides eventually became spalled.

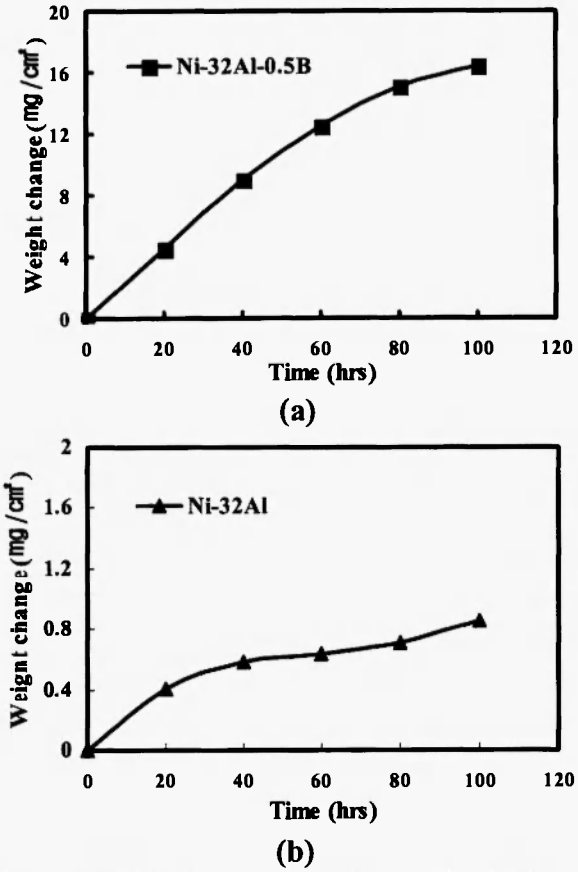

Fig. 2: Weight changes per unit area after isothermal oxidation at 1100°C in air flowing at the rate of 70cc/min., a) Ni-32at.%Al and b) Ni-32at.%Al-0.5at.%B

The temperature dependency of oxidation behaviors of individual nickel aluminides such as NiAl and Ni_3Al has been studied extensively /9-13/, but not many attempts have been made to illuminate the oxidation behaviors of two phase NiAl+Ni_3Al nickel aluminides.

Micrographs of surface oxides formed in the Ni-32at.%Al two phase nickel aluminide are shown in Fig. 3. After 5 minutes at 1100°C general surface oxidation of NiO on the Ni_3Al phase and $NiAl_2O_4$ on the NiAl matrix was observed as shown in Fig. 3a) and 3b). On further exposure for 30 minutes at 1100°C

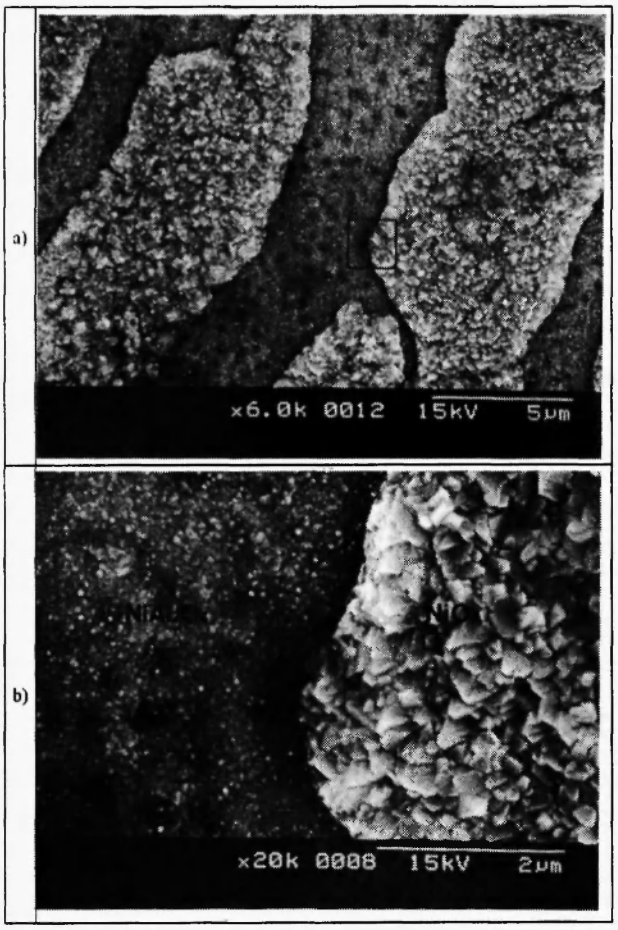

Fig. 3: SEM micrographs of Ni-32at.%Al specimens after oxidation for 5 minutes at 1100°C in air flowing at the rate of 70cc/min. a) top view, b) enlarged image of □ in a)

surface oxides began to spall as shown in Fig. 4a) and general growth of the surface oxides as shown in Fig. 4b) as well as a trace of θ-Al_2O_3 phase formation as indicated in Fig. 4c) were observed. After exposure for

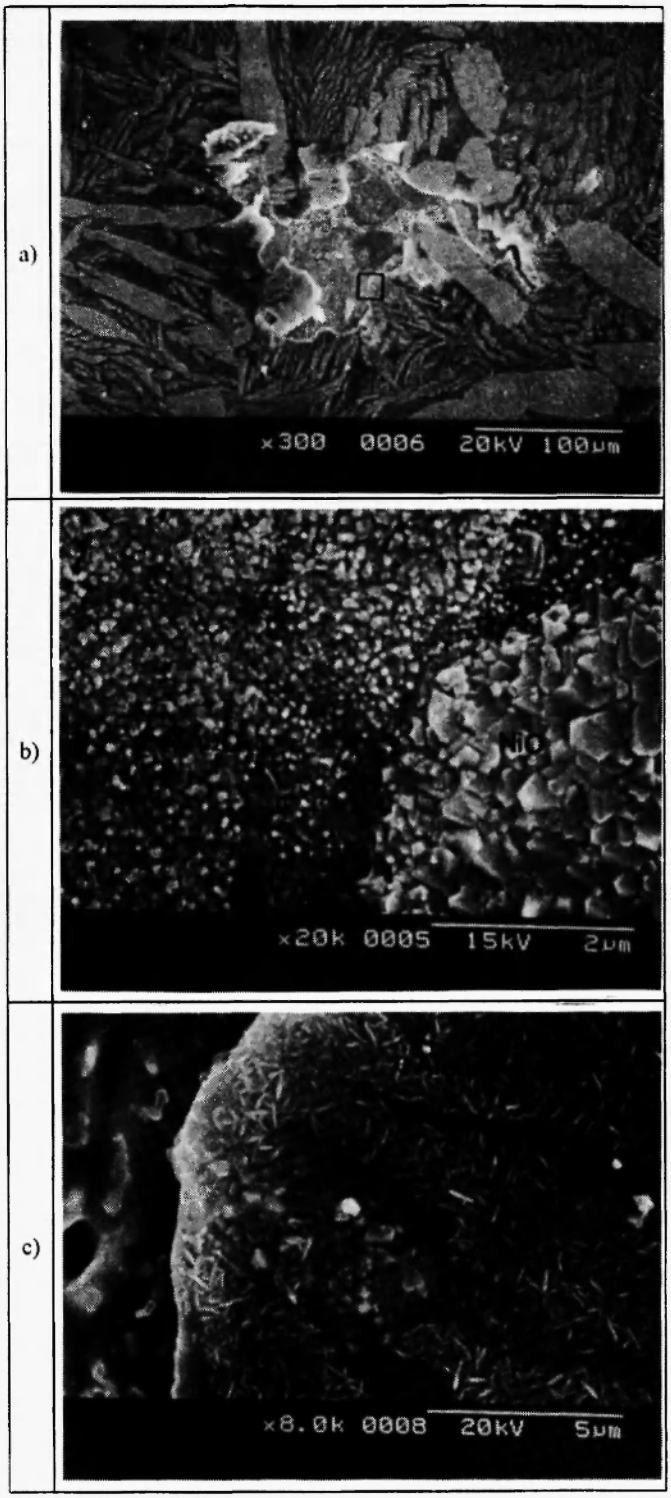

Fig. 4: SEM micrographs of Ni-32at.%Al specimens after oxidation for 30 minutes at 1100°C in air flowing at the rate of 70cc/min. a) top view, b) enlarged image of matrix in a), c) enlarged image of □ in a)

40 hours at 1100°C, all the surface oxides transformed into α-Al_2O_3 phase and extensive spallation was observed as shown in Fig. 5a). Cross sectional microstructure of Ni-32at.%Al alloy after exposure for 40 hours at 1100°C is shown in Fig. 5b) and the results from the EDS analysis are summarized in Table 1.

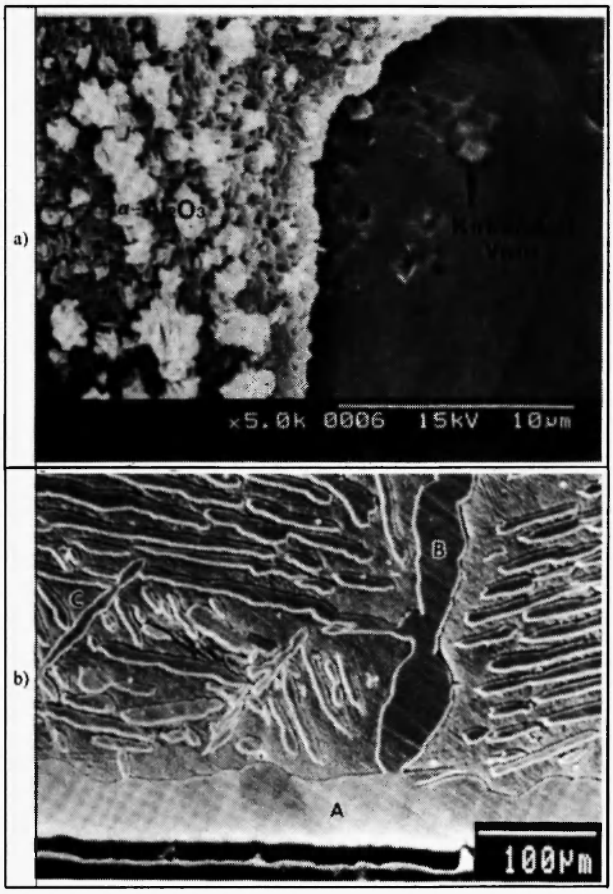

Fig. 5: SEM micrographs of Ni-32at.%Al specimens after oxidation for 40hours at 1100°C in air flowing at the rate of 70cc/min. a) top view, b) cross sectional view

These indicated that in Ni-32at.%Al alloy a continuous supply of Al from the matrix NiAl phase was provided resulting in the formation of continuous layer of Ni_3Al phase at the surface.

In the case of Ni-32at.%Al-0.5at.%B alloy, a very complex microstructure was observed in the grain boundary region as shown in Fig. 1d), in that martensitic β-NiAl was present in the matrix and several phases of Ni_3Al, Ni solid solution, and borides were present at the grain boundary region /7,8/. Accordingly more complex oxidation behaviors were expected especially within the grain boundary region.

After 5 minutes at 1100°C Ni-32at.%Al-0.5at.%B alloy showed distinct difference in the oxide formed on the surface depending upon the location as shown in Fig. 6a). Within the grain boundary region, NiO phase was observed near the grain boundary where Ni_3Al phase was present, while at the center area of the grain boundary region, where a combination of γ(Ni) phase and boride were present, θ-Al_2O_3 phase was observed as shown in Fig. 6b). General precipitation of γ-Ni_3Al phase and NiO phase was observed in the matrix as shown in Fig. 6c). On further oxidation for 30 minutes at 1100°C, a much clearer difference in the oxidation behavior between the matrix and the grain boundary region, as well as extensive spallation, were noticed (Fig. 6d)). Within the grain boundary region, NiO, $NiAl_2O_4$ and θ-Al_2O_3 phases were observed toward the center and the intermediate $NiAl_2O_4$ phase was believed to form through the solid state interaction between the NiO phase and θ-Al_2O_3 phase (Fig. 6e)), which was previously reported by other investigators /9/. Formation of θ-Al_2O_3 phase in the NiO-spalled area was observed in the matrix as shown in Fig. 6f). After exposure for 40 hours at 1100°C, extensive spallation

Table 1

EDS results from oxidized surfaces shown in Fig. 5b) and Fig. 7a)

area	a) Ni-32at.%Al (in Fig. 5b))	b) Ni-at.32%Al-0.5at%B (in Fig. 7a))
A	25.99	96.46
B	28.11	12.28
C	36.52	36.33

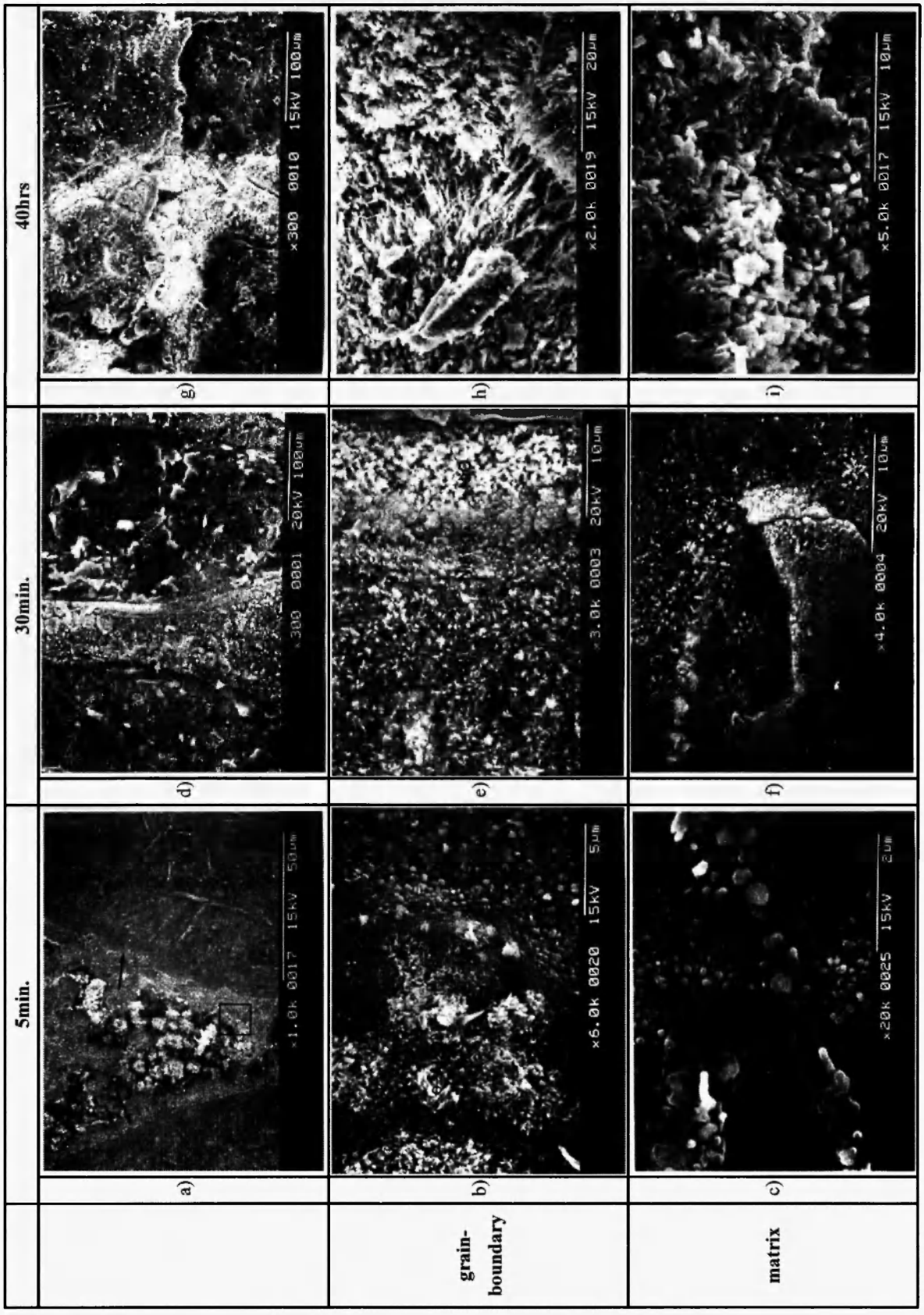

Fig. 6: SEM micrographs of Ni-32at.%Al-0.5at%B specimens after oxidation for various times at 1100°C in air flowing at the rate of 70cc/min., a) "g" represents grain boundary, b) enlarged image of □ in a)

was noticed as shown in Fig. 6g) and α-Al_2O_3 phase prevails all over the surface (Fig. 6i)). Whisker type θ-Al_2O_3 oxide in the grain boundary region was present as shown in Fig. 6h).

Cross-sectional microstructure of Ni-32at.%Al-0.5at.%B alloy after exposure for 40 hours at 1100°C and the results from the EDS analysis are shown in Fig. 7. In Ni-32at.%Al-0.5at.%B alloy, crack separating the surface oxide and the matrix was observed and surface oxidation progresses by penetrating the surface Ni_3Al layer in the Ni-32at.%Al-0.5at.%B alloy. Comparing Al contents between the "B" area and the "C" area in Fig. 7a) (Table 1), Al content in the "B" area is much reduced, indicating that extensive depletion of Al from the matrix due to surface oxidation has occurred. From the EDS results obtained from different regions in Fig 7 it is believed that $NiAl_2O_4$ phase is present in region 1 and is undergoing a transformation into α-Al_2O_3 phase through a reaction of $3NiAl_2O_4 + 2Al \rightarrow 4Al_2O_3 + 3Ni$ /9/. α-Al_2O_3 phase was identified in regions 2 and 3, and a Kirkendall void due to Al depletion /14/ was observed in region 4. Connection of the Kirkendall voids between regions 2 and 3 could eventually lead to crack development for spallation.

Results from X-ray diffraction analysis on the surface oxides formed after various oxidation exposure on both intermetallic compounds are summarized in Fig. 8a) and 8b), respectively, confirming the phases mentioned above.

SUMMARY AND CONCLUSIONS

Oxidation behaviors of two phase NiAl+Ni_3Al intermetallic compounds and the effect of boron addition at 1100°C were examined. Intermetallic compounds with and without boron addition showed general parabolic oxidation behavior, but addition of boron to the two phase NiAl+Ni_3Al intermetallic compounds deteriorated the oxidation resistance. An accelerated oxidation along the thin layer of Ni_3Al at the grain boundary region observed in the Ni-32at.%Al-0.5at.%B intermetallic compound could be attributed to the poor oxidation resistance, compared

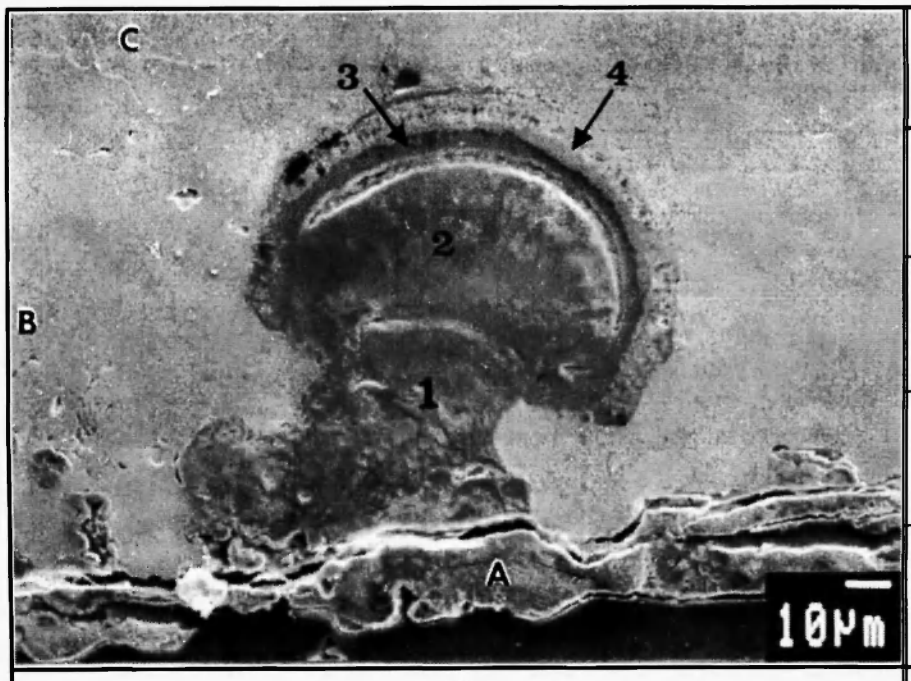

a)

Area	Al (at.%)
1	83.63
2	98.78
3	97.28
4	74.29

b)

Fig. 7: Ni-32at.%Al-0.5at.%B specimens oxidized for 40hrs at 1100°C in air flowing at the rate of 70cc/min. a) SEM cross-sectional micrographs, b) EDS results

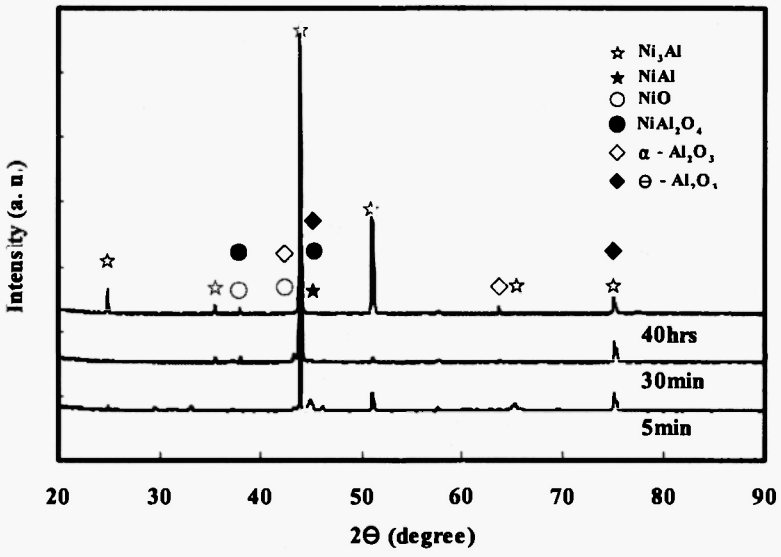

(a)

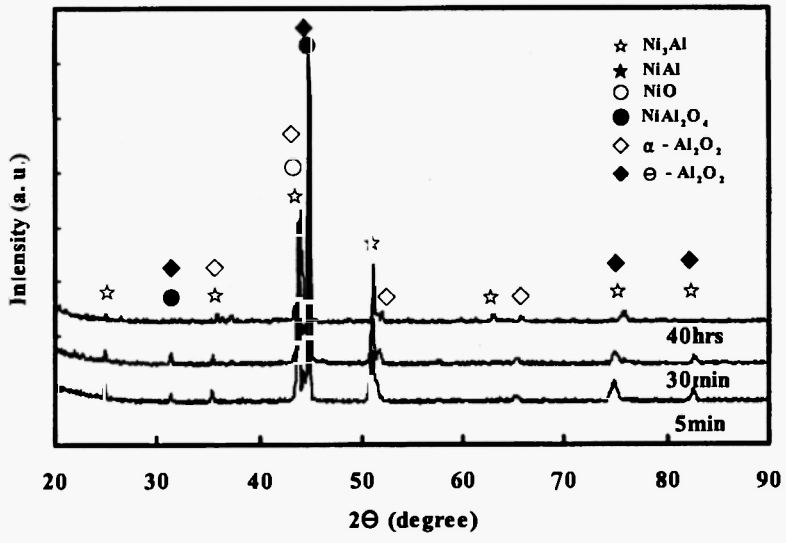

(b)

Fig. 8: X-ray diffraction pattern of specimens oxidizied for 5min., 30min. and 40hrs at 1100°C in air flowing at the rate of 70cc/min. a) Ni-32at.%Al alloy and b) Ni-32at.%Al-in air flowing at the rate of 70cc/min. a) Ni-32at.%Al alloy and b) Ni-32at.%Al-00.5at.%B alloy

with the Ni-32at%Al intermetallic compound showing no grain boundary Ni_3Al phase. In the Ni-32at%Al-0.5at%B intermetallic compound, quite complex oxidation behaviors involving several types of oxide such as NiO, $NiAl_2O_4$, θ-Al_2O3, α-Al_2O3 phases were observed in the early stage depending upon the location at the grain boundary regions.

REFERENCE

1. K.C. Russell and J.W. Edington, *Mat. Sci. J.*, **6**, 20 (1972).
2. R. Moskovic; *Journal of Materials Science*, **13**, 1901 (1978).
3. K. Ishida, R. Kainuma, N. Ueno, and T.

Nishizawa, *Metall. Trans.*, **22A**, 441 (1991).
4. S. Ochiai, I. Yamada and Y. Kojima; *J. Japan Inst. Metals*, **54**(3), 301 (1990).
5. J.H. Lee, B.H. Choe, and H.M. Kim, *Mat. Sci. & Eng.*, **A152**, 253 (1992).
6. J.H. Lee, S.Y. Lee, Z.H. Lee, and H.M. Kim, *High Temp. Matl. Proc.*, **18**(3), 122 (1999).
7. J.H. Lee, J.H. Lee, Z.H. Lee, and H.M. Kim, *High Temp. Matl. Proc.*, **18**(3), 145 (1999).
8. S.Y. Lee and J.U. Bae, *J. Korean Inst. Metals and Materials* **16**(4), 55 (1998) .
9. S.C. Choi, Ph.D. Thesis, Sung Kyun Kwan University, 1996.
10. J.L. Smialek and R. Gibala, *Met. Trans.*, **14A**, 2143 (1983).
11. J.K. Doychak, J.L. Smialek and T.E. Mitchell, *Proc. Int. Cong. Metall. Corros.* **1**, 35 (1984).
12. G.C. Rybicki and J.L. Smialek, *Oxid. Met.*, **31**, 275 (1989).
13. J.K. Doychak and M. Ruhle, *Oxid. Met.*, **31**, 431 (1989).
14. M. M. Janssen and G. D. Rieck, *Trans. AIME*, **239**, 1372 (1967).